Enzyme-Catalyzed Regioselective Modification of Starch Nanoparticles

Soma Chakraborty,[†] Bishwabhusan Sahoo,[†] Iwao Teraoka,[†] Lisa M. Miller,[‡] and Richard A. Gross*,[†]

NSF Center for Biocatalysis and Bioprocessing of Macromolecules, Othmer Department of Chemical and Biological Science and Engineering, Polytechnic University, Six Metrotech Center, Brooklyn, New York 11201, and National Synchrotron Light Source, Brookhaven National Laboratory, Upton, New York 11973

Received June 11, 2004; Revised Manuscript Received September 29, 2004

ABSTRACT: The selective esterification of starch nanoparticles was performed using as catalyst *Candida antartica* Lipase B (CAL-B) in its immobilized (Novozym 435) and free (SP-525) forms. The starch nanoparticles were made accessible for acylation reactions by formation of Aerosol-OT (AOT, bis(2-ethylhexyl)sodium sulfosuccinate) stabilized microemulsions. Starch nanoparticles in microemulsions were reacted with vinyl stearate, ϵ-caprolactone, and maleic anhydride at 40 °C for 48 h to give starch esters with degrees of substitution (DS) of 0.8, 0.6, and 0.4, respectively. Substitution occurred regioselectively at the C-6 position of the glucose repeat units. Infrared microspectroscopy (IRMS) revealed that AOT-coated starch nanoparticles diffuse into the outer 50 μm shell of catalyst beads. Thus, even though CAL-B is immobilized within a macroporous resin, CAL-B is sufficiently accessible to the starch nanoparticles. When free CAL-B was incorporated along with starch within AOT-coated reversed micelles, CAL-B was also active and catalyzed the acylation with vinyl stearate (24 h, 40 °C) to give DS = 0.5. After removal of surfactant from the modified starch nanoparticles, they were dispersed in DMSO or water and were shown to retain their nanodimensions.

Introduction

Starch is an abundant, inexpensive, naturally occurring polysaccharide. It is biocompatible, biodegradable, and nontoxic, so it can be used as biocompatible implant materials and drug carriers.[1−6] Literature reports describe the use of chemically modified forms of starch for sustained drug delivery systems. For example, epichlorohydrin cross-linked high amylose starch was used as a matrix for the controlled release of contramid.[1] A complex of amylose, butan-1-ol, and an aqueous dispersion of ethylcellulose was used to coat pellets containing salicylic acid to treat colon disorders.[2] Starch has also been used as a carrier for phenethylamines,[3] acetylsalicylic acid,[4] and estrone.[5] Hydrogels composed of starch/cellulose acetate blends were reported as possible bone cements.[6] While starch-based biomaterials appear promising, scientific challenges remain to be solved. For example, it would be advantageous if starch esters used as matrices for drug delivery could be prepared so that they are modified at selected positions of the glucose residues (i.e., at only the primary or secondary positions). This is difficult due to the presence of three hydroxyl groups per glucose residue each in different chemical environments. Furthermore, to solubilize starch for homogeneous modification, polar aprotic solvents such as dimethyl sulfoxide are needed. For example, to modify the primary (6-O) hydroxyl sites of amylose, starch was heterogeneously persilylated, the persilylated derivative in carbon tetrachloride was acylated with an anhydride, and then the silyl protecting groups were removed.[7]

Previous work has investigated the use of enzymes to regioselectively modify polysaccharides under mild conditions. Hydroxyethylcellulose (HEC) particles were suspended in dimethylacetamide and acylated with vinyl stearate using *Candida antartica* Lipase B (CAL-B) as catalyst. After 48 h, a product with degree of substitution (DS) 0.1 was formed.[8] Lipase-catalyzed modification of HEC in film or powder form by reaction with ϵ-caprolactone (CL) gave low-DS HEC-*g*-PCL copolymers.[9] Problems associated with these strategies are use of (i) polar aprotic solvents that strip critical water from enzymes lowering their activities[10] and (ii) heterogeneous reaction conditions that restrict the modification of large particles and films to a small fraction of the substrate residing at the surface. To overcome the use of polar aprotic solvents, enzymes have been incorporated within reverse micelles using the anionic surfactant aerosol-OT [AOT, bis(2-ethylhexyl)sodium sulfosuccinate]. AOT forms thermodynamic water droplets surrounded by a surfactant monolayer in oil (isooctane). Water entrapped within the reverse micelles resembles the polar pockets in cells.[11] Incorporation of enzymes within reverse micelles soluble in nonpolar media facilitates productive collisions and reactions between enzymes and nonpolar substrates. Several types of lipase-catalyzed reactions in AOT/isooctane have been studied.[12] Dordick and co-workers incorporated proteases from *Subtilisin carlsberg* and *Bacillus licheniformis* within AOT-coated reverse micelles.[13] Although the enzymes within reverse micelles were active for the acylation of amylose in film and powder form, the inability of AOT-coated enzyme to diffuse into the bulk of these substrates limited modification of films and powders to surface regions.

Nanoparticles, nanospheres, and nanogels are used as building blocks for nanoscale construction of sensors, tissues, mechanical devices, and drug delivery systems. For the latter, carriers with nanodimensions are not detected by the reticuloendothelial system so they circulate for longer times. For medical applications, nanoparticles constructed from poly(lactic acid), poly-

[†] Polytechnic University.
[‡] Brookhaven National Laboratory.
* Corresponding author. E-mail: rgross@poly.edu.

10.1021/ma048842w CCC: $30.25
Published on Web 12/13/2004

(glycolic acid),[14−16] poly(alkyl cyanoacrylate),[17,18] 2-hydroxyethyl acrylate−poly(ethylene glycol)diacrylate copolymers,[19] poly(L-lysine)-*g*-polysaccharides,[20] and poly(vinylpyrrolidone)[21] have been reported. Starch microspheres were studied for the delivery of insulin via the nasal system.[22]

To overcome previous difficulties in the enzymatic esterification of polysaccharides and to prepare a family of structurally and dimensionally well-defined nanoparticles from a natural material, a new idea was explored. That is, starch nanoparticles were incorporated into reverse micelles stabilized by AOT. A key discovery was that the nanodimensions of AOT-coated starch particles and their solubility in nonpolar media such as toluene allowed their diffusion to sites within the pores of the physically immobilized lipase catalyst Novozym 435 at which esterification of starch occurred. The acyl donors included vinyl esters of fatty acids differing in chain length, maleic anhydride, and ϵ-caprolactone. Motivations for selecting these acyl donors were as follows: (i) increase starch hydrophobicity, (ii) introduce both carboxylate side chains and sites for free radical cross-linking, and (iii) form polyester grafts. Nuclear magnetic resonance experiments gave the degree of substitution (DS) and regioselectivity of esterification reactions. The influence of the reaction temperature, time, and structure of the acyl donor on the progress of esterification reactions was studied. IR microspectroscopy revealed the extent that AOT-coated starch nanoparticles diffuse through the macroporous structure of the physically immobilized lipase catalyst Novozym 435. Dynamic light scattering showed the size distribution of AOT-coated reverse emulsions of starch nanospheres both prior to and after starch modification reactions. Furthermore, dynamic light scattering confirmed that the nanodimensions of modified starch nanoparticles were retained after they had been stripped of AOT and dispersed in water or DMSO.

Material and Methods

General Chemicals and Procedure. Starch nanoparticles (Ecosphere) of average size 40 nm were prepared by Ecosynthetix and provided as a gift. The method used to prepare starch nanoparticles was described in detail elsewhere.[23] All chemicals and solvents were of analytical grade, purchased from Aldrich Chemical Co. Inc., and were used as received unless otherwise noted. ϵ-Caprolactone (CL) was a gift from Union Carbide Co. Novozym 435 and SP-525 were gifts from Novozymes. Toluene and CL were dried over calcium hydride and distilled under reduced pressure in a nitrogen atmosphere. AOT was dried in vacuo (16 h, 25 °C, 1 mmHg) prior to use. Novozym-435 was dried over P_2O_5 in vacuo (16 h, 25 °C, 0.5 mmHg) prior to use. Molecular sieves (4 Å, 4−8 mesh size) were purchased from Aldrich Chemical Co. Inc. and dried for 24 h at 160 °C prior to use.

Instrumental Methods. ^{1}H and ^{13}C-DEPT-135 NMR spectra were recorded at 25 °C on a DPX300 spectrometer at 300 and 75.13 MHz, respectively (Bruker Instruments, Inc.). The proton (^{1}H) and carbon (^{13}C)-DEPT-135 NMR chemical shifts in parts per million (ppm) were referenced relative to tetramethylsilane (TMS). To perform the ^{1}H and ^{13}C NMR experiments, 8.0 and 20.0 wt % of samples were dissolved in their respective solvents. FTIR spectra were recorded using a Thermo Nicolet Magna 760 FTIR spectrometer using potassium bromide (KBr) disks prepared from powdered samples mixed with dry KBr in the ratio of 1:100 (sample:KBr). The spectra were recorded in a absorbance mode from 4000 to 400 cm^{-1} at a resolution of 8 cm^{-1}. The particle size distribution of starch nanoparticles was characterized at 25 °C by using a N4 Plus particle sizer (Beckman-Coulter) with a He−Ne laser (λ = 632.8 nm). Samples for the measurement were prepared by dispersing nanoparticles at 1% (w/w) in their respective solvents. Unmodified starch nanoparticles were dispersed in DMSO as well as in water. Starch nanoparticles modified with either CL or vinyl stearate were dissolved in DMSO. Maleic anhydride-modified starch nanoparticles were dissolved in water. DMSO and aqueous solution samples were filtered through hydrophobic and hydrophilic PTFE filters, respectively (both 0.2 μm pore size; Millipore). Filtered samples were collected into dust-free fluorometer cells (10 × 10 mm). Starch nanoparticles incorporated in the reverse micelles of AOT (AOT:starch = 2:1 w/w) and dispersed in toluene were measured without filtration. N4 Plus measures an autocorrelation function of the light scattering intensity at different scattering angles and converts it into a distribution of the apparent particle diameter d, assuming that the light scattering comes from spherical particles independently making diffusional motion. The distribution is weighted by the scattering intensity of each particle of the relevant size at the scattering angle used.

To prepare the samples for IR microspectroscopy (IRMS), Novozym beads were recovered from the reaction vessel after 24 h reaction between starch nanoparticles and vinyl stearate at 40 °C in toluene. Beads were washed with toluene and then with water to remove the particles from their surface. Washed beads were dried in vacuo (16 h, 25 °C, 1 mmHg). These beads were embedded in paraffin wax and microtomed at room temperature into sections with a thickness of 12 μm. Sections were mounted on a BaF_2 disk and the IR microspectra were recorded using a Perkin-Elmer Spectrum Spotlight infrared microscope equipped with a motorized $x-y$ stage and an MCT-A detector. The IR microscope was coupled to a Spectrum One FTIR spectrometer. Data were collected from 4000 to 700 cm^{-1} in transmission mode, 32 scans/pixel, 4 cm^{-1} spectral resolution, and 6.25 μm pixel resolution. Control spectra of starch, AOT, and Novozym 435 beads were also collected under the same conditions. Additional details of the general methods and data analysis are described elsewhere.[24]

Incorporation of Starch Nanoparticles within Reverse Micelles of AOT/Isooctane/H_2O Microemulsions. A concentrated aqueous solution of starch nanoparticles (0.25 g/mL) was added dropwise with vigorous stirring to 50 mL of 0.1 M AOT/anhydrous isooctane solution in a round-bottom flask capped with a rubber septum. Throughout this process the solution remained clear, and phase separation did not occur. This gave reverse micelles of AOT-coated starch nanoparticles in isooctane. Isooctane from the modified nanoparticles was removed under reduced pressure by using a rotavaporator. The AOT-coated micelles were further dried (30 °C, 6 h, 30 mmHg). A similar procedure was adopted to incorporate starch nanoparticles in reverse micelles of CTAB/chloroform and TritonX-100/toluene where, in place of AOT/isooctane, the surfactant/solvent systems used were CTAB/chloroform and TritonX-100/toluene.

Incorporation of Nonimmobilized *Candida antartica* Lipase B (CALB) within AOT-Coated Starch Nanoparticles. Starch nanoparicles (2.2 g) and SP-525 (1.1 mL, protein content 0.022 g) were added to 7.7 mL of deionized water. Incorporation of starch nanoparticles within reverse micelles of AOT/isooctane/H_2O microemulsions was performed exactly as described above, except that SP-525 was present in the aqueous solution.

Acylation of AOT-Coated Starch Nanoparticles with Vinyl Stearate. Vinyl stearate was used as the acylating agent for the hydrophobic modification of starch nanoparticles. The starch nanoparticles (2.2 g, 0.0135 mol of glucose units) coated with surfactant was transferred to a 100 mL round-bottomed flask. Dry toluene (50 mL), vinyl stearate (12.63 g, 0.0407 mol), and Novozym 435 (0.22 g) were added to the reaction vessel. The molar ratio of acylating agent to glucose residues was 3 to 1. The reactions were performed in the presence of molecular sieves at six different temperatures (25, 30, 35, 40, 50, and 60 °C) for 48 h with stirring. Control reactions were performed as above but in the absence of Novozym 435 at 40 and 60 °C. Reactions were terminated by

filtration to remove the enzyme and sieves. Then, toluene was removed under reduced pressure. To remove AOT, the product was suspended in a mixture of water and methanol (50 mL, 1:1 v/v) at 25 °C for 30 min with magnetic stirring. The suspended nanoparticles were separated by filtration, and then, to remove unreacted acylating agent, they were transferred into a beaker containing 50 mL of cold chloroform. The suspension was magnetically mixed at 25 °C for 30 min, separated by filtration, and the residual solvent was removed under reduced pressure. The purified products were characterized by different spectroscopic techniques. For the 48 h reaction with vinyl stearate, the product obtained is of DS 0.8, and the results of NMR studies for this product were as follows: ^{1}H NMR in DMSO-d_6 (δ in ppm): 5.27 [C1-*H*, m, 1H], 4.22 [C6-*H*, m, 2H], 3.74 [C2-*H*, C4-*H*, m, 2H], 3.42 [C3-*H*, C5-*H*, m, 2H], 2.18 [−O(C=O)CH_2−, t, 2H], 1.53 [−O(−C=O)CH$_2$CH_2−, q, 2H], 1.32 [−(CH_2)$_9$−, s, 18H], 0.72 [−CH_3, t, 3H]. ^{13}C-DEPT in DMSO (showed the carbon signals for the sugar ring) (δ in ppm): δ 73.68 (C3), 72.54 (C2), 72.18 (C5, unmodified starch unit), 72.13 (C4), 66.74 (C5, modified starch unit), 65.04 (C6, modified starch unit), 61.07 (C6, unmodified starch unit).

Maleation of AOT-Coated Starch Nanoparticles. Starch nanoparticles (2.2 g, 0.0135 mol of glucose units) and dry toluene (50 mL) were transferred to a 100 mL round-bottomed flask. To this was added maleic anhydride (1.323 g, 0.0135 mol), Novozym 435 (0.22 g), and hydroquinone (3 mg, free radical inhibitor). The reactions were performed at 40 °C for 48 h with magnetic stirring. The workup procedure of the reaction was identical to that for the acylation of starch nanospheres with vinyl stearate. The purified product was characterized by different spectroscopic techniques. NMR spectral data of starch maleate nanoparticles (DS 0.4, 48 h reaction) were as follows: ^{1}H NMR in D_2O (δ in ppm): 5.85 [H$_a$, bs, 1H, maleic anhydride unit proton −(O=C−CH_a=CH$_b$-COOH)], 6.65 [H$_b$, bs, 1H, maleic anhydride unit proton −(O=C−CH$_a$=CH_bCOOH)], 5.52 [C1-*H*, m, 1H], 4.36 [C6-*H*, m, 2H], 4.04−3.51 [C2-*H*, C3-*H*, C4-*H*, m, 3H], 3.02 [C5-*H*, m, 1H] (see Figure S-2 in Supporting Information for more details on peak signals and assignments). ^{13}C-DEPT spectrum (starch signals, in D_2O, δ in ppm): δ 145.28 and 120.23 (C$_a$ and C$_b$, −C$_a$=C$_b$−), 72.43 (C4), 73.88 (C3), 72.91 (C2), 72.83 (C5, unmodified starch unit), 69.56 (C5, modified starch unit), 61.91 (C6, unmodified starch unit), 66.12 (C6, modified starch unit).

Reaction of AOT-Coated Starch Nanoparticles with ϵ-Caprolactone (CL). The reaction procedure was identical to that for the maleation of starch nanoparticles, except that CL (4.40 mL, 4.536 g, 0.0405 mol) was used in place of maleic anhydride. The purified product is characterized by different spectroscopic techniques. NMR spectral data of caprolactone modified starch nanoparticles (DS 0.6, 48 h reaction) were as follows: ^{1}H NMR in DMSO (δ in ppm): 5.52 [C1-*H*, m, 1H], 4.21 [CH_2−O−C(O), caprolactone methylene proton, m], 4.13 [C6-*H*, m, 2H], 3.52−3.86 [C2-*H*, C3-*H*, C4-*H*, C5-*H*, m, 4H], 2.21 [−C(O)CH_2−, of caprolactone units], 1.58 [m, methylene protons and CH_2OH of capralactone units], 1.32 [m, other methylene protons of capralactone units] (see Supporting Information for more detailed information on peak signals and assignments, Figure S-3). ^{13}C-DEPT (starch signals in DMSO, δ in ppm): δ 73.68 (C3), 72.54 (C2), 72.18 (C5, unmodified starch unit), 72.13 (C4), 70.21 (C5, modified starch unit), 65.01 (C6, modified starch unit), 61.07 (C6, unmodified starch unit).

Acylation of Starch Nanoparticles Using SP-525. The acylation of AOT-coated starch nanoparticles with vinyl stearate was performed as described above, except that CAL-B was incorporated directly within the microspheres instead of being introduced into the reaction in its immobilized form (i.e., Novozyme 435).

Results and Discussion

1. Synthesis and Structural Analysis of Modified Starch Nanoparticles. 1.1. Preparation of Surfactant-Coated Starch Nanoparticles. A key idea of this work was to solubilize starch nanospheres by their incorporation in reverse micelles. By encapsulation of starch nanospheres with a surfactant, it was hoped they might disperse in a low-polarity medium, rendering them accessible to both an enzyme immobilized on the walls of a macroporous support and an acyl donor. To explore this concept, the loading of starch nanospheres within surfactant stabilized reverse micelles was investigated. The surfactant−solvent systems used were AOT (sodium bis(2-ethylhexyl) sulfosuccinate)/isooctane, CTAB (cetyltrimethylammonium bromide)/chloroform and Triton X-100 (polyoxyethylene-10-isooctylphenyl ether)/toluene. These surfactants were selected on the basis of their previous use for other applications of solubilized enzymes in reversed micelles.[26,27] To load the reverse micelles, a concentrated (0.25 g/mL) aqueous solution of starch nanospheres was added to the different surfactant/solvent pairs. The percent incorporation of starch in the nanospheres was determined on the basis of the amount of starch nanoparticles that could be added to the surfactant/solvent system prior to formation of a cloudy phase-separated mixture.

Table 1. Percent Incorporation of Starch Nanoparticles in Different Surfactant Systems

entry	surfactant[a]	nature	solvent	starch nanoparticles incorporated (%)[b]
1	AOT	anionic	isooctane	50
2	CTAB	cationic	chloroform	40
3	Triton X-100	neutral	toluene	10

[a] The surfactant concentration in the organic solvent was 0.1 M. [b] Starch nanoparticles/surfactant (w/w) × 100.

The results in Table 1 show that the AOT/isooctane microemulsion system gave the highest percent incorporation of starch nanoparticles in reverse micelles. To isolate the AOT-coated starch nanoparticles, the isooctane was removed under reduced pressure. Previous studies in our laboratory showed that toluene was a preferred organic medium in which to perform Novozym 435-catalyzed transesterification reactions.[28] Hence, AOT-coated starch nanospheres were dispersed in toluene and evaluated as acyl acceptors for a series of lipase-catalyzed starch modification reactions.

1.2. Lipase-Catalyzed Acylation of AOT-Coated Starch Nanoparticles. Novozym 435 is a biocatalyst consisting of lipase B from *Candida antarctica* (CAL-B) immobilized onto a poly(methacrylate) macroporous resin (Lewatit VP OC 1600). It has been shown that the average pore size of Novozym 435 beads is about 100 nm.[25] An initial concern in using this catalyst for modifying AOT-coated starch nanospheres was whether the AOT-coated nanospheres would have access to CAL-B within the beads. This would require the diffusion of the nanospheres within pores of Novozym 435. The ability of Novozym 435 to modify the starch nanospheres was first tested. Later, the size of AOT-coated starch nanospheres and its ability to diffuse into the catalyst beads are described.

The acyl donors selected include (i) fatty acid vinyl esters that when esterified to starch greatly increase its hydrophobicity, (ii) maleic anhydride that ring-opens, giving carboxylic acids and sites for free-radical cross-linking or grafting, and (iii) ϵ-caprolactone that can ring-open to form polyester grafts of various chain lengths (Scheme 1). The reaction between vinyl stearate and AOT-coated starch nanoparticles was performed for 24 h, at 40 °C, with a 3:1 mol/mol ratio of vinyl stearate to glucose residues. The products obtained were analyzed by ^{1}H and ^{13}C NMR spectra. Peak positions and assign-

Scheme 1. Reactions between AOT-Coated Starch Nanoparticles with Different Acylating Agents[a]

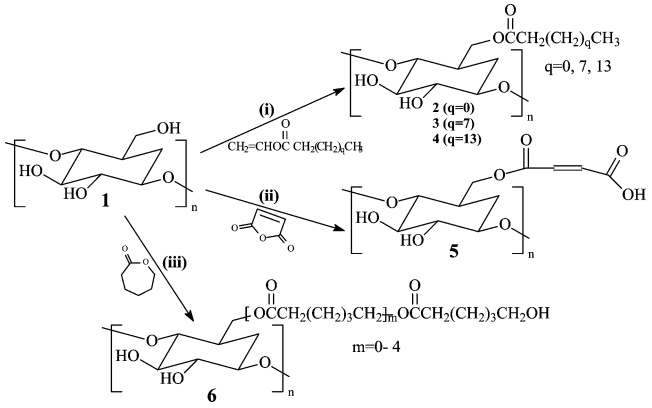

[a] Conditions: Novozym 435 (1% protein w/w), toluene, 40 °C, 48 h; (i) ratio glucose units to vinyl ester 1:3 mol/mol, (ii) glucose units to maleic anhydride 1:1 mol/mol, (iii) glucose units to ϵ-caprolactone 1:3 mol/mol.

ments of NMR spectra are listed in the Experimental Section and are consistent with that expected. Proton NMR (300 MHz, DMSO-d_6) signals with peaks at 5.27, 4.22, 3.74, and 3.42 ppm are due to the protons of C1, C6, (C2/C4), and (C3/C5), respectively (see Figure S-1). Other ^{1}H NMR signals at 2.18, 1.53, 1.32, and 0.72 ppm were assigned to hydrogens of the stearate moiety (see Figure S-1). Determination of DS by ^{1}H NMR was based on the relative intensities of peaks at 5.27 ppm (proton on C1) and 1.53 (CH_2 of stearate). The intensities of the peaks were determined by integrating them. Exchange with D_2O caused the disappearance of the 2OH and 3OH protons that, otherwise, overlap with the proton of C1 at 5.27 ppm. Comparison of the DEPT-135 spectra (Figure 1) of the native starch nanoparticles and the vinyl stearate-modified starch nanoparticles (48 h reaction, DS = 0.8) shows that acylation of glucose residues caused (i) the signal at 72.18 ppm for C5 of unmodified glucose units to shift upfield to 66.74 ppm and (ii) the peak at 61.07 ppm for C6 of the unmodified substrate

Table 2. Effect of the Reaction Temperature on the Acylation with Vinyl Stearate of AOT-Coated Starch Nanospheres[a]

entry	temp (°C)	reaction efficiency (%)[b]	DS
1	25	7.0	0.2
2	30	10.0	0.3
3	35	17.0	0.5
4	40	27.0	0.8 ± 0.06[c]
5	50	30.0	0.9
6	60	30.0	0.9

[a] Reaction time: 24 h; starch nanoparticles:Novozym 435 = 10:1 (w/w); ratio of acylating agent to glucose units 3:1 mol/mol. [b] [Vinyl stearate esterified to starch/vinyl stearate in the reaction] × 100. [c] Reaction performed in triplicate to determine the standard deviation.

to shift downfield to 65.04 ppm. The other ring carbons at 73.68 (C3), 72.54 (C2), and 72.13 ppm (C4) were found at almost identical positions in the starting substrate and the modified product. The peaks at 72.18 and 61.07 ppm in the product spectrum correspond to C5 and C6 of unmodified sugar units. Thus, the DEPT-135 spectra in Figure 1 show that Novozym 435 catalysis of starch nanosphere acylation with vinyl stearate is selective for C6. In other words, only the hydroxyl attached to the C6 of glucose units participates in ester bond formation.

1.3. Influence of Reaction Temperature. Using vinyl stearate as the acyl-donor, Novozym 435-catalyzed esterification of AOT-coated starch nanospheres were conducted at temperatures from 25 to 60 °C (see Table 2).

By increasing the reaction temperature from 25 to 50 °C but keeping all other reaction variables constant, the efficiency of the reaction increased from 7.0 to 30% and the DS increased from 0.2 to 0.9. Further increasing the reaction temperature from 50 to 60 °C caused the reaction efficiency to decrease. The reaction at 40 °C was performed in triplicate to determine the standard deviation. For control reactions performed at 40 and 60 °C but without enzyme, no acylation of the product was observed. This supports that the esterifications were catalyzed by the enzyme and not by non-enzyme-

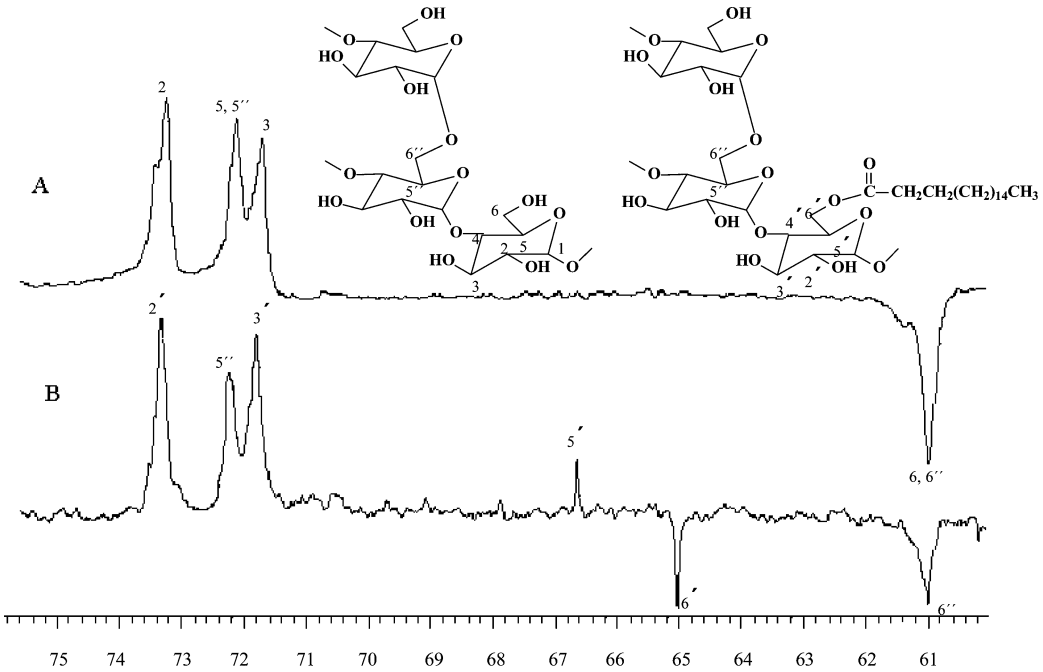

Figure 1. Expanded region of DEPT-135 (75 MHz, DMSO-d_6) spectra that shows the carbon signals for the sugar units of (A) native starch nanoparticles and (B) vinyl stearate modified starch nanoparticles with DS = 0.8.

Table 3. Effect of the Acylating Agent Chain Length on Its Reactivity[a]

entry	acylating agent	reaction efficiency (%)	DS
1	vinyl stearate	27.0	0.8
2	vinyl decanoate	13.0	0.4
3	vinyl propionate	3.0	0.1
4	vinyl acetate	no reaction	0.0

[a] Reaction time: 24 h; starch nanoparticles to Novozym 435 is 10:1 (w/w); acylating agent to glucose units 3:1 mol/mol.

mediated chemical reactions. The results of experiments at reaction temperatures from 25 to 40 °C were used as a basis for selecting the temperature for other studies in this work. The experiments at 50 and 60 °C were performed only after most of the studies described in this paper had already been completed.

1.4. Effect of Substrate Chain Length on Starch Acylation. Vinyl-activated fatty acids with 2, 3, 10, and 18 carbons were investigated as acyl donors (see Table 3). No esterification was detected by NMR analysis using vinyl acetate (two-carbon chain length). By increasing the fatty acid chain length from 3 to 10 and 10 to 18 carbons, the reaction efficiency increased from 3.0 to 13.3% and 13.0 to 27.0%, respectively. Hence, the reactivity increased by using fatty acid acyl donors of longer chain length. This observation is consistent with earlier studies that describe a preference of CAL-B for hydrophobic substrates such as when the Novozym 435-catalyzed ring-opening polymerization of ω-pentadecalactone was found to proceed more rapidly than ϵ-caprolactone.[29] To determine whether vinyl ester activation was needed, stearic acid was used in place of vinyl stearate. Unfortunately, esterification was not observed with steric acid.

1.5. Acylation of AOT-Coated Starch Nanoparticles with Maleic Anhydride. The reaction between maleic anhydride and AOT-coated starch nanoparticles was performed for 24 h, at 40 °C, with a 1:1 mol/mol ratio of maleic anhydride to glucose residues. The NMR peak positions and assignments for maleic anhydride esterified starch nanoparticles are listed in the Experimental Section. The DS was calculated from the ^{1}H NMR (300 MHz) by comparing the relative intensity of peaks at 5.85 (O═C−CH_a═CH_bCOOH) and 5.52 ppm (proton at C1). Relative intensities of the peaks were determined by integrating them. As above, the only changes in the DEPT-135 spectrum after reaction with maleic anhydride (product DS 0.4) were new signals at 69.56 and 66.12 for C5 and C6, respectively. The upfield shift of C5 (by 3.27 ppm) and downfield shift for C6 (by 4.21 ppm) in combination with no other changes in the spectrum for carbons of the glucose ring shows that esterification with maleic anhydride occurred selectively at the C6 positions of glucose units.

The apparent higher reactivity of vinyl stearate than maleic anhydride is consistent with the preference of Novozym 435 for hydrophobic substrates of long chain length rather than polar substrates of small ring size (see Table 3). Furthermore, the activation energy of maleic anhydride ring-opening is likely increased by the development of charge−charge repulsion between the developing carboxylate group and the negatively charged AOT surfactant molecules. Nevertheless, maleation to DS 0.4 builds into the nanoparticles a substantial quantity of both unsaturated moieties for cross-linking and pendant carboxylic acids that alter the particle charge density.

1.6. Acylation of AOT-Coated Starch Nanoparticles with ϵ-Caprolactone (CL). The reaction between ϵ-caprolactone (CL) and AOT-coated starch nanoparticles was performed for 24 h, at 40 °C, with a 3:1 mol/mol ratio of CL to glucose residues. The peak positions and assignments are listed in the Experimental Section. Analysis of the DEPT-135 spectrum of products as above showed that CL units were selectively esterified at the C6 position of glucose units. Similar regioselectivity was observed for the ethyl glucoside-initiated ring-opening polymerization of CL catalyzed by Novozym 435.[30] The DS of products was determined by ^{1}H NMR from the relative intensity of peaks at 5.52 (proton of C1) and 2.18 ppm (−C(O)−CH_2). The degree of polymerization (DP) was determined from the relative intensity of the caprolactone methylene protons (CH_2−O−C(O)) at 4.46 ppm and the methylene protons (CH_2−O−C(O)) at the C6 ring position of esterified glucose residues. Relative intensity of the peaks was determined by integrating them. The results of CL DS and DP as a function of reaction time are given below.

1.7. Reaction Progress with Time. The time course for acylations of AOT-coated starch nanoparticles with vinyl stearate, CL, and maleic anhydride are shown in Figure 2 and discussed below. Acylation with vinyl stearate begins after a 2 h lag period and by 24 h reached DS 0.7. Extending the reaction time to 48 h showed at most an increase in DS to 0.8.

The lag period observed for stearate acylation is likely due to the immiscibility of hydrophobic vinyl stearate and hydrophilic starch molecules. However, once a low degree of stearate ester formation occurs, the solubility of vinyl stearate in the hydrophobically modified starch nanoparticles increases, thus accelerating the reaction. In contrast, a lag period was not observed for the reaction with CL. This is consistent with a relatively higher miscibility of CL than vinyl stearate with the starch nanoparticles (see Figure S-4, Supporting Information, for the effect of reaction time on substitution from 12 to 24 h). While stearate substitution at 4 h was only 0.2, CL substitution had already reached 0.4 and an average degree of polymerization (DP) of 1.7. By 12 h, the degree of CL and stearate substitution were 0.6 (DP = 2.0) and 0.4, respectively. With an increase in the reaction time from 12 to 48 h, neither the DS nor the DP increased substantially beyond 0.6 and 2.0, respectively. However, addition of another 3 equiv of CL per glucose residue to the reaction system at 24 h resulted in oligo(CL) side chains with an average DP of 5 units with no further increase in the DS. It follows that with further addition of CL longer graft lengths will result. Reports by others that have attempted to form starch-*g*-PCL by ring-opening polymerizations using chemical catalysts (e.g., stannous octanoate) have similarly reported the formation of starch-*g*-polycaprolactone.[31] However, unlike previously described graft polymerizations using chemical catalysts where polycaprolactone emanates randomly from the primary and secondary hydroxyl positions, starch-*g*-polycaprolactone from lipase catalysis has grafts that uniformly begin by attachment to the primary hydroxyl groups of glucose residues.

Maleation of starch nanoparticles occurred slowly. By 12 h the DS was 0.1, and it increased to 0.4 by 48 h. The reactions with maleic anhydride were performed in the presence of hydroquinone to avoid the possibility

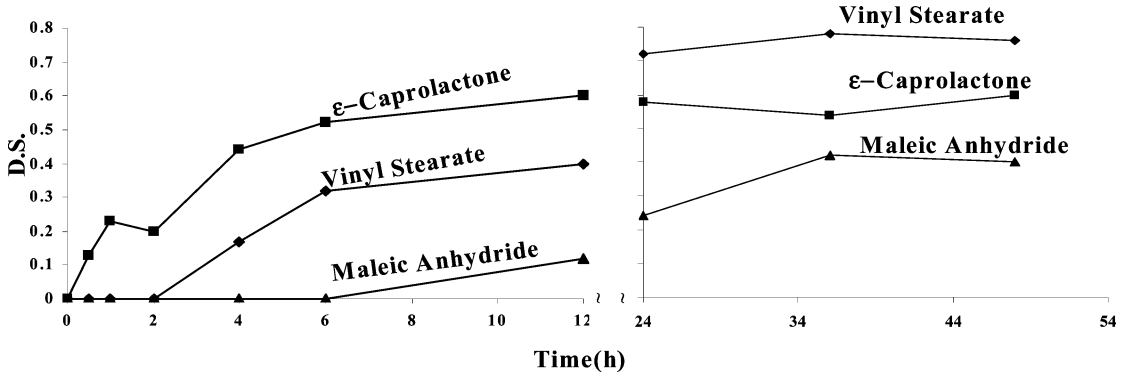

Figure 2. Effect of reaction time on degree of substitution for the reaction of starch with different acylating agents; starch (glucose residues):vinyl stearate 1:3 mol/mol, starch:maleic anhydride 1:1 mol/mol, starch:ϵ-capralactone 1:3 mol/mol.

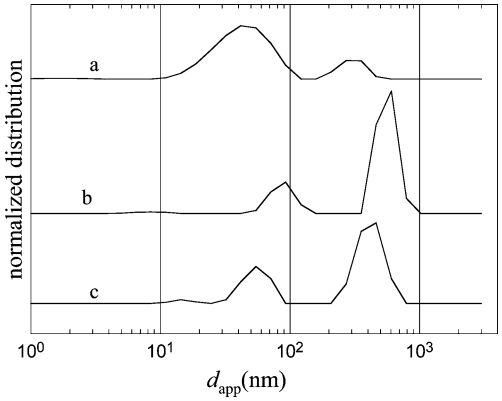

Figure 3. Distribution of particle diameter d for (a) unmodified, (b) stearate-modified (DS = 0.8), and (c) ϵ-caprolactone-modified (DS = 0.6) starch nanoparticles in DMSO recorded at the scattering angle of 28.2°. Each curve is normalized by the total area of the peaks above the baseline.

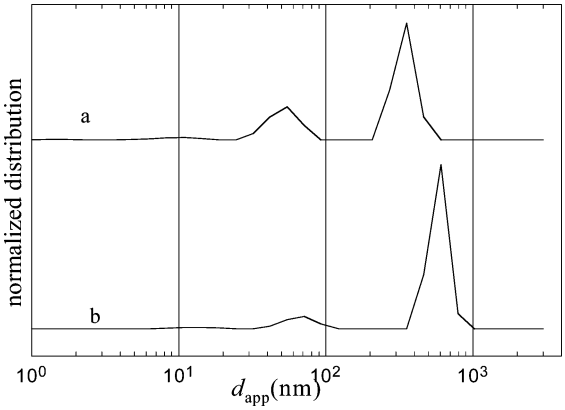

Figure 4. Distribution of particle diameter d for (a) unmodified and (b) maleic anhydride-modified starch nanoparticles (DS = 0.4) in water recorded at 30°.

of free-radical side reactions. Furthermore, when succinic anhydride was used in place of maleic anhydride, its reactivity was similarly slow.

2. Characterization of Unmodified and Modified Starch Nanoparticles by Light Scattering. It was hoped that the method used to modify the starch nanoparticles could result in nanosize products. Dynamic light scattering (DLS) experiments were performed to determine the particle size distribution of the starting material and products. Prior to the analysis, the modified nanoparticles were treated to remove AOT and other residual reactants (see Experimental Section). Figure 3 shows the particle size distributions of the unmodified and modified starch nanoparticles in DMSO recorded at the scattering angle of 28.2°.

Also, these measurements were performed in DMSO at 21.5° and 64.3°. Common to the three scattering angles is distributions of the unmodified and modified nanoparticles have peaks at almost the same locations. Unmodified nanoparticles exhibit two prominent peaks at around 45 and 300 nm. The smaller particles are ascribed to isolated nanoparticles and the larger particles to their aggregates. In Figure 3a, the peak area for the smaller particles is about 3 times as large as that for the larger particles. There is a third weak peak at around 2 nm. In general, the scattering intensity by suspended particles is roughly proportional to the product of their mass concentration and the molar mass of each particle. Therefore, the lower peak height at 300 nm indicates that these large particles are present in negligibly small amounts. The predominant hydrodynamic diameter of unmodified starch nanoparticles in DMSO is 45 nm. This result is in a good agreement with the SEM micrograph given by the nanoparticle supplier (not shown).

DLS analysis of vinyl stearate-modified nanoparticles (DS = 0.8) shows that each of the peaks, including the third weak peak, shifted to a larger size (Figure 3b). Furthermore, the peak area for the larger particles is 3 times as large as the one for the smaller particles. The changes in the distribution indicate that modification caused the nanoparticles to exist mostly as aggregates of several particles and the aggregates of $d_{app} \cong 300$ nm to aggregate further. Nevertheless, the modified nanoparticles still remain dispersed in DMSO.

For the CL-modified nanoparticles (DS = 0.6), the shifts in the peak positions of the two major peaks are not as large as those for the vinyl stearate-modified starch. Furthermore, the increase of the peak area for the larger particles is less. Hence, modification with CL resulted in particles with a weaker attractive interaction compared with the vinyl stearate modification. Noteworthy is that all the samples passed through a 0.2 μm filter. Therefore, particles of $d_{app} \cong 300$ nm are dynamic aggregates that are in equilibrium with the smaller particles.

Figure 4 shows the size distribution of unmodified and maleic anhydride-modified starch nanoparticles dispersed in water, obtained at 30.2°. The results at 23° and 62.6° are almost identical. Unmodified starch nanoparticles show two prominent peaks at 50 and 350 nm, both slightly larger than their counterparts in DMSO. Unlike in DMSO, the larger particles have a greater peak area than do the smaller particles. Thus, the relative population of the larger particles in water

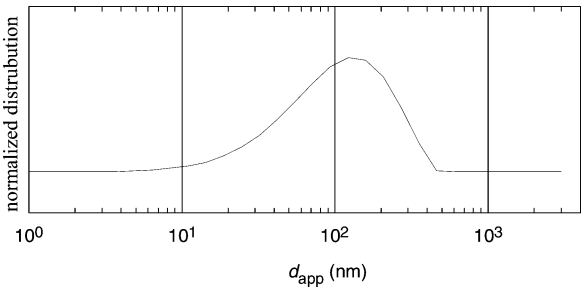

Figure 5. Distribution of particle diameter d of AOT-coated starch nanoparticles in toluene recorded at 30° in toluene.

is not negligible. A third peak was also observed at around 10 nm. Apparently, compared with DMSO, water has a poorer ability to disperse starch nanoparticles. Modification with maleic anhydride resulted in shifts of the three peaks to larger particle diameters with growth of the area for larger particles.

In addition to the analysis of modified starch nanoparticles after they were isolated and stripped of AOT, light scattering experiments were also performed to characterize unmodified AOT-coated starch nanoparticles. Light scattering studies in toluene at 30° showed these particles have a unimodal size distribution in the range from 5 to 350 nm (Figure 5).

Reverse micelles of AOT without starch nanoparticles were not observed. The critical micelle concentration of AOT is far above the concentration used in sample preparation. Thus, the low end of the distribution in Figure 5 represents a suspension that holds only one or two 40 nm starch nanoparticles or their fragments. In contrast, the high end of the distribution is ascribed to aggregates that contain many 40 nm nanoparticles. Unlike DMSO and water, the environment of toluene and AOT limits the area of contact between starch and the solvent, which disfavors the presence of isolated nanoparticles.

3. Diffusion of Starch Nanoparticles into Novozym 435 Beads. Previous work showed that the average pore size of Novozym 435 beads is about 100 nm.[25] Furthermore, CAL-B is not distributed throughout the entire Novozym 435 bead; it is located in an outer shell with a thickness of 80−100 μm for beads with an average diameter of about 500 μm.[25] In this work, we determined whether AOT-coated nanospheres diffuse within Novozym 435 beads. If this is not possible, reactions of starch nanospheres would be restricted to outer regions of Novozym 435 beads, thus largely limiting the fraction of enzyme available for catalysis of starch acylation. The extent of penetration by AOT-coated starch nanoparticles within catalyst beads was investigated with infrared microspectroscopy. Novozym 435 beads were withdrawn at 12 h from a reaction between starch nanoparticles and vinyl stearate at 40 °C. These beads were embedded in paraffin, sectioned to a thickness of 12 μm with a microtome, and deposited on BaF_2 disks. Infrared images were collected from bead cross sections. To determine the IR spectral features unique to starch, spectra were recorded for Novozym 435 (CAL-B loaded on the PMMA macroporous matrix polymer) and nonmodified starch nanospheres (Figure 6A). For Novozym 435, the C=O stretching mode between 1720 and 1740 cm^{-1} is due to the matrix polymer,[25] so this spectral range was integrated in each pixel of the infrared image to determine the matrix polymer distribution in the bead (Figure 6B). Similarly,

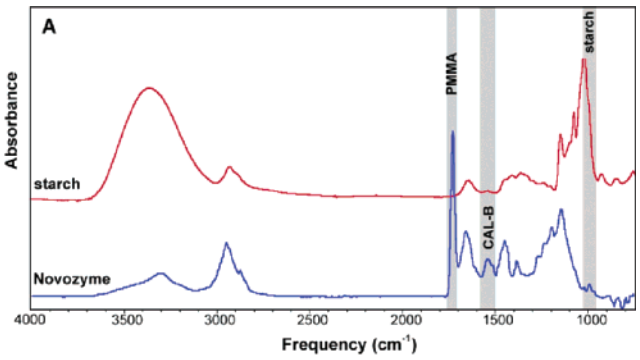

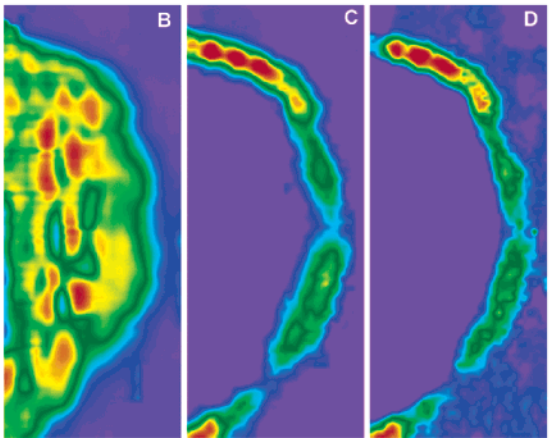

Figure 6. Distribution of modified AOT-coated starch nanoparticles within Novozym 435 as observed by infrared microscopy (IRMS). (A) Control spectra of pure starch nanoparticles (top) and recovered Novozym 435 beads (bottom). Spectral peaks unique to the matrix polymer, CAL-B, and starch are highlighted in gray. The distribution in bead cross sections of the matrix polymer (PMMA), CAL-B, and starch nanospheres are shown in (B), (C), and (D), respectively.

the amide II protein band from 1500 to 1575 cm^{-1} was integrated to determine the CAL-B distribution (Figure 6C), and the C−O stretching mode between 1025 and 1058 cm^{-1} was integrated to determine the starch distribution in the bead (Figure 6D). It was found that both the CAL-B protein content and the starch nanoparticle content were localized within an outer shell of the bead. Since the starch nanoparticles penetrated ~50 μm into the bead, and CAL-B is located in the outer 80−100 μm region of beads, the AOT-coated starch nanoparticles penetrate well within the beads where they encounter much of the available enzyme. This is reasonable since light scattering showed the average diameter of AOT-coated starch nanospheres was 5−350 nm (Figure 5), and the average pore diameter of the beads is 100 nm.[25] Once inside the pore, CAL-B and starch molecules are in intimate contact so that starch hydroxyl groups can react with enzyme activated ester complexes. This observation explains why Novozym 435 is so effective at modifying starch nanoparticles.

4. Incorporation of CALB within AOT-Coated Starch Nanospheres. An alternative to modification of starch nanoparticles by immobilized CAL-B is catalysis by nonimmobilized or "free" CAL-B. Free CAL-B was incorporated into reversed micelles during its preparation in AOT/isooctane/water (see Experimental Section). This was accomplished by mixing an aqueous solution of SP-525 (as-received) and starch nanospheres with AOT in isooctane (see above). The resulting AOT-coated starch nanospheres containing CAL-B were

reacted with vinyl stearate (3 mol equiv per glucose unit) in toluene at 40 °C for 24 h to give a product with DS 0.5. Under similar reaction conditions except using Novozym 435 as the catalyst, the product DS was 0.7. Furthermore, analysis of the regioselectivity of acylation by DEPT-135 NMR analysis showed that free CALB incorporated within the micelles was also regioselective for the C6 position. Thus, the use of free CAL-B is a reasonable alternative to that of Novozym 435.

Summary of Results

Starch nanoparticles were incorporated into AOT-coated reverse micelles that dissolved in toluene. Light scattering analysis of a suspension of these particles in toluene showed that, at the low end of the size distribution, the aggregates have one or two 40 nm starch nanoparticles. At the high end of the distribution, aggregates that contain many 40 nm nanoparticles were found. By forming dispersions of these starch nanoparticle clusters in toluene, starch molecules become highly accessible to nonpolar substrates and the lipase CAL-B that is immobilized within pores of beads. Furthermore, toluene promotes the activity of the CAL-B for acylation reactions. Previous work that attempted lipase-catalyzed acylations of starch or other polysaccharides used large particles or films where only a small fraction of the polymer on surface layers was accessible to the enzyme. The other alternative of forming a solution of the polysaccharide in polar aprotic solvents such as DMSO is flawed since DMSO and other polar aprotic solvents that dissolve polysaccharides strip critical water from the enzyme catalyst, rendering it with little or no activity. When AOT-coated dispersions of starch nanoparticles in toluene were exposed to physically immobilized CALB (Novozym 435), acylations of ϵ-caprolactone (CL), vinyl stearate, and maleic anhydride were successfully accomplished. The reactions were performed at 40 °C for up to 48 h. DEPT-135 spectra of the products showed that starch acylation occurred regioselectively at C6 positions of glucose units. Using vinyl stearate at 40 °C, the product degree of substitution reached 0.8. The acylation with CL occurred most rapidly so that, by 12 h, the degree of CL substitution was 0.6 (DP = 2.0). In comparison, by 12 h, the degree of starch substitution with vinyl stearate and maleic anhydride was 0.4 and 0.1, respectively. By increasing the concentration of CL available in the reaction, starch-*g*-polycaprolactone was formed with grafts that uniformly emanate from the primary hydroxyl groups of glucose residues. Infrared microspectroscopy (IRMS) showed that AOT-coated starch nanoparticles can diffuse into the outer 50 μm shell of catalyst beads. Since CAL-B is located in the outer 100 μm shell of catalyst beads, starch and acylating agents are all in close proximity promoting esterifications. Studies by dynamic light scattering proved that, after isolation of acylated particles with surfactant removal, nanodimension products could be redispersed in DMSO or water.

Acknowledgment. We are grateful to the members of the NSF I/UCRC for Biocatalysis and Bioprocessing of Macromolecules for their financial support, encouragement, and stimulating discussions. We acknowledge the generous gift of enzyme from Novozymes and Ecosynthetix for the starch nanoparticles.

Supporting Information Available: ^{1}H NMR spectra and the graph of the degree of substitution with respect to time. This material is available free of charge via the Internet http://pubs.acs.org.

References and Notes

(1) Lenaerts, V.; Moussa, I.; Dumoulin, Y.; Mebsout, F.; Chouinard, F.; Szabo, P.; Mateese, M. A.; Cartilier, L.; Marchessault, R. *J. Controlled Release* **1998**, *53*, 225.
(2) Vandamme, Th. F.; Lenourry, A.; Charrrueau, C.; Chaumeil, J.-C. *Carbohydr. Polym.* **2002**, *48*, 219.
(3) Zikha, A.; Weiner, B. Z.; Tahan, M. *J. Med. Chem.* **1972**, *15*, 410.
(4) Sjoholm, I.; Laakso, T.; Stjarnkvist, P. *J. Pharm. Sci.* **1986**, *76*, 134.
(5) Won, C.; Chu C.; Yu, T. *Carbohydr. Polym.* **1997**, *32*, 239.
(6) Pereira, C. S.; Cunha, A. M.; Reis, R. L. *J. Mater. Sci.: Mater. Med.* **1998**, *9*, 825.
(7) Roesser, D. S.; McCarthy, S. P.; Gross, R. A.; Kaplan, D. L. *Macromolecules* **1996**, *29*, 1.
(8) Cheng, H. N.; Gu, Q.-M. *ACS. Symp. Ser. 840*, 203.
(9) Li, J.; Xie, W.; Cheng, H. N.; Nickol, R. G.; Wang, P. G. *Macromolecules* **1999**, *32*, 2789.
(10) Klibanov, A. M. *TIBTECH* **1997**, *15*, 97.
(11) *Membrane Mimetic Chemistry: Characterizations and Applications of Micelles, Microemulsions, Monolayers, Bilayers, Vesicles, Host−Guest Systems and Polyions*; Wiley: New York, 1982; p 60.
(12) Schwugner, M. J.; Stickdorn, K.; Schomäcker, R. *Chem. Rev.* **1995**, *95*, 849.
(13) Bruno, F. F.; Akkara, J. A.; Ayyagari, M.; Kaplan, D. L.; Gross, R.; Swift, G.; Dordick, J. S. *Macromolecules* **1995**, *28*, 8881.
(14) Murthy, S. K.; Qi, Z.; Remsen, E. E.; Wooley, K. L. *Polym. Mater. Sci. Eng.* **2001**, *84*, 1073.
(15) Govender, T.; Stolnik, S.; Garnett, M. C.; Illum, L.; Davis, S. S. *J. Controlled Release* **1999,** *57*, 171.
(16) Perez, C.; Sanchez, A.; Putnam, D.; Ting, D.; Langer, R.; Alonso, M. J. *J. Controlled Release* **2001**, *75*, 211.
(17) Couvreur, P.; Kante, B.; Lenaerts, V.; Scailteur, V.; Roland, M.; Speiser, P. *J. Pharm. Sci.* **1998**, *69*, 199.
(18) Fontana, G.; Licciardi, M.; Mansueto, S.; Schillaci, D.; Giammona, G. *Biomaterials* **2001**, *22*, 2857.
(19) McAllister, K.; Sazani, P.; Adam, M.; Cho, M. J.; Rubinstein, M.; Samulski, R. J.; DeSimone, J. M. *J. Am. Chem. Soc.* **2002**, *124*, 15198.
(20) Maruyama, A.; Ishihara, T.; Kim, J.; Sung, W.; Akaike, T. *Colloids Surf. A: Physiochem. Eng. Aspects* **1999**, *153*, 439.
(21) Madan, T.; Munshi, N.; De, T. K.; Maitra, A.; Sarma, P. U.; Aggarwal, S. S. *Int. J. Pharm.* **1997**, *159*, 135.
(22) Björk, E.; Edman, P. *Int. J. Pharm.* **1990**, *62*, 187.
(23) Patent No. WO 00/40617, 2000.
(24) Mei, Y.; Miller, L.; Gao, W.; Gross, R. A. *Biomacromolecules* **2003**, *4*, 70.
(25) Bru, R.; Sánchez-Ferrer, A.; García-Carmona, F. *Biochem. J.* **1995**, *310*, 721.
(26) Menger, F. M.; Yamada, K. *J. Am. Chem. Soc.* **1979**, *101*, 6731.
(27) O'Connor, C. J.; Sun, C. Q.; Lai, D. T. *Surfactant Sci. Ser.* **2003**, *109*, 171.
(28) Kumar, A.; Gross, R. A. *Biomacromolecules* **2000**, *1*, 133.
(29) Kumar, A.; Kalra, B.; Dekhterman, A.; Gross, R. A. *Macromolecules* **2000**, *33*, 6303.
(30) Bisht, K. S.; Deng, F.; Gross, R. A. *J. Am. Chem. Soc.* **1998**, *120*, 1363.
(31) Choi, E. J.; Kim, C. H.; Park, J. K. *Macromolecules* **1999**, *32*, 7402.

MA048842W